International Journal of Dental Research and Allied Sciences
2021, Volume 1, Issue 2, Page No: 88-95

Available online at: www.tsdp.net

ISSN: 3062-3502

Original Article

Biomechanical Impact of Implant Diameter and Bone Quality on Single-Crown Restorations: A Finite Element Study

Juan Rodríguez[1], Zoey Stewart[2], María González[1]*

[1]Department of Periodontics and Oral Medicine, University of Michigan School of Dentistry, Ann Arbor, MI, USA.
[2]Department of Restorative Dentistry & Endodontics, Faculty of Dentistry, University of Puthisastra, Phnom Penh, Cambodia.

***E-mail** ✉ mgonzalez99@outlook.com

Received: 06 August 2021; **Revised:** 17 November 2021; **Accepted:** 18 November 2021

ABSTRACT

The performance of implant-supported restorations is strongly influenced by both the implant diameter and the surrounding bone density. This research aimed to examine how these two parameters affect stress distribution when subjected to vertical and 30° oblique loading. A finite element analysis was performed using dental implants of a constant length of 6.5 mm, but with different diameters (Ø3.3, Ø3.5, Ø3.75, Ø4.0, Ø4.25, and Ø4.75 mm). Each implant was positioned axially and restored using a 2 mm high straight transepithelial abutment for a single-tooth prosthesis. Four bone density conditions—Type IV, III, II, and 0-I—were modeled based on a simplified mandibular segment. A 200 N force was applied vertically and at a 30° inclination to the occlusal surface, located 11 mm above the implant platform, and the equivalent Von Mises stresses in bone were evaluated. The highest stress value appeared in Type IV bone with the Ø3.3 implant (235 MPa), whereas the lowest was found in Type 0-I bone with the Ø4.75 implant (41 MPa). Across all diameters, improved bone density corresponded with reduced stress levels. Increasing the implant diameter produced a similar, but more pronounced, reduction in bone stress. Implant diameter plays a major role in minimizing bone stress, as wider implants distribute loads more efficiently.

Keywords: Biomechanics, Finite element modeling, Single-tooth implant, Short implant

How to Cite This Article: Rodríguez J, Stewart Z, González M. Biomechanical Impact of Implant Diameter and Bone Quality on Single-Crown Restorations: A Finite Element Study. Int J Dent Res Allied Sci. 2021;1(2):88-95. https://doi.org/10.51847/58EwTgX0Xs

Introduction

Finite element analysis (FEA) serves as a computational approach to predict the stress patterns generated within an implant and the surrounding bone. During mastication, both axial and bending loads are transmitted through the implant fixture to the bone. The way these forces are distributed affects the mechanical stability of the implant and adjacent bone tissues. Numerous variables influence how stresses are conveyed to bone [1], including the loading direction, bone-implant contact quality, implant geometry, surface characteristics, prosthetic configuration, and host bone properties [1, 2]. For instance, certain implant designs may produce excessive or insufficient stresses around the peri-implant bone, potentially compromising its stability [1, 3].

The success of an implant largely depends on how efficiently these stresses are transferred to the supporting bone [1]. Two fundamental determinants of biomechanical performance in implant-supported restorations are implant diameter and bone quality [1, 2]. Using finite element simulations, some researchers demonstrated that implant diameter has a significant effect on stress distribution and suggested that wider implants could help reduce localized bone stress [4]. However, their work did not include variable bone density conditions and was limited to Type 0-I bone.

Other researchers reported that the maximum stress concentrations occur at the implant neck. They also

found that as implant diameter increased, both peak stress values and stress concentration zones in cortical bone decreased, while longer implants improved stress distribution within trabecular bone [5]. Prior research has indicated that increasing implant diameter produces a greater reduction in bone stress compared to increasing implant length [6]. Stress accumulation typically occurs in the cortical region regardless of implant design, meaning that simply increasing implant length is not sufficient to offset the effects of crown height [7, 8].

Eazhil *et al*. further demonstrated, through finite element models, that Von Mises stress concentrates near the implant collar [9]. Their results confirmed that implant diameter is a more decisive factor than implant length in dissipating stress, with wider implants showing better load distribution.

Bone density at the implant site and the resulting primary stability also play critical roles in treatment outcomes [10]. According to Rabel *et al*. primary stability is determined by a combination of bone quality and quantity, implant geometry, and surgical technique [11]. Azcárate-Velázquez *et al*. used FEA to evaluate how different bone types affect stress patterns under compressive and oblique loading in two implant designs [12]. They reported that lower bone density led to unfavorable stress concentration and cortical bone overload, especially under oblique loading.

Several investigations have evaluated short implants as single-unit restorations in posterior areas [13, 14]. Nevertheless, Mezzomo *et al*. found in a meta-analysis that implants ≤8 mm were linked to increased marginal bone loss, higher failure rates, and biological complications [15]. Conversely, a recent meta-analysis revealed that the crown-to-implant (C/I) ratio in single and nonsplinted implants does not significantly increase biological or mechanical complications [16]. Guljé *et al*. observed that even a high C/I ratio (2.14 ± 0.42) in 6-mm single-unit implants did not correlate with bone loss or prosthetic issues [17].

Further biomechanical and clinical investigations are needed to clarify the parameters influencing the longevity of single-unit restorations supported by short implants. The current study therefore focuses on evaluating the effect of implant diameter on stress transfer to bone, incorporating various bone quality types to simulate a broader range of clinical scenarios.

Materials and Methods

For this analysis, a simplified representation of the mandible was modeled as a cylindrical block measuring Ø15.5 mm in diameter and 15.5 mm in height **(Figures 1a–1f)**.

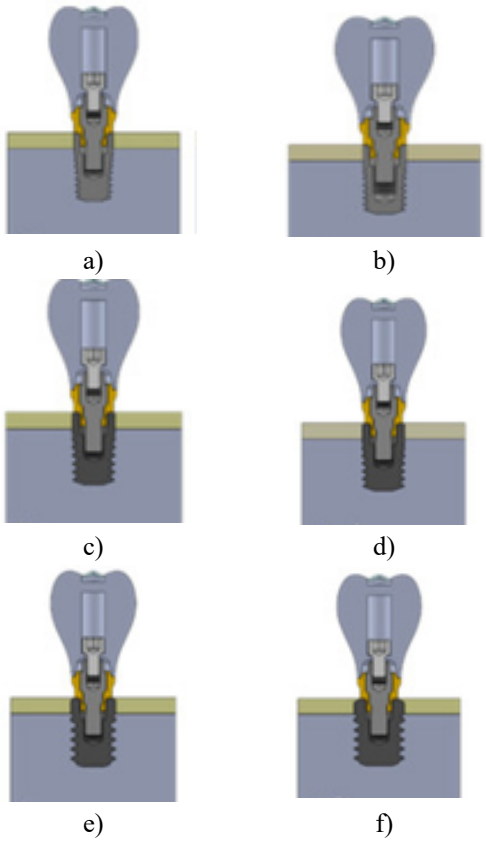

Figure 1. (1-a) 3D view with an Ø3.3 implant in Type III bone under axial positioning. (1-b) Ø3.5 implant in Type III bone. (1-c) Ø3.75 implant in Type III bone. (1-d) Ø4.0 implant in Type III bone. (1-e) Ø4.25 implant in Type III bone. (1-f) Ø4.75 implant in Type III bone.

The classification of bone types used in this study followed the system by Anitua *et al*. [2, 10], derived from the model proposed by Lekholm and Zarb [18]. This approach considered both bone density (in Hounsfield Units) and cortical bone thickness, obtained through BTI Scan software (BTI Biotechnology Institute, Vitoria, Spain). According to this method, six bone categories were defined: 0, I, II, II, III, IV, and V.

The simulations were performed under four bone conditions, described as follows:

- Case 1 **(Figure 2a)** – Type IV bone, density 400–<500 HU, with a 0.5-mm cortical layer surrounding cancellous bone [2, 10].
- Case 2 **(Figure 2b)** – Type III bone, density 550–<850 HU, and a cortical shell of 1.5 mm [2, 10].
- Case 3 **(Figure 2c)** – Type II bone, density 850–<1000 HU, with a 3-mm thick cortical layer [2, 10].
- Case 4 **(Figure 2d)** – Type 0-I bone, density exceeding 1000 HU, and cortical thickness of 8 mm [2, 10].

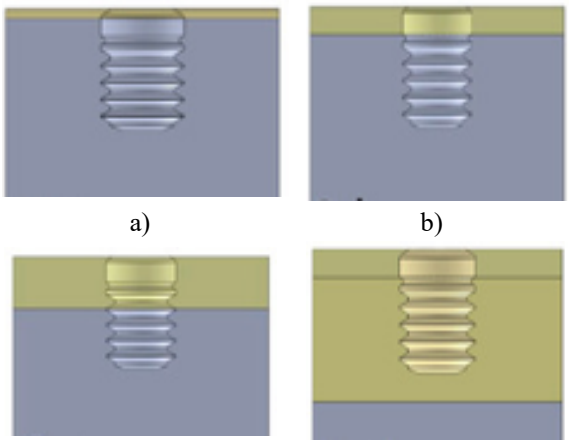

a) b) c) d)

Figure 2. (2-a) Case 1: Type IV bone. (2-b) Case 2: Type III bone. (2-c) Case 3: Type II bone. (2-d) Case 4: Type 0-I bone.

Each implant was modeled as being completely osseointegrated. To simplify the analysis and maintain symmetry, the helical thread geometry was replaced with a revolved thread form. This geometric adjustment allowed better consistency among the test cases, ensuring that minute structural details did not disproportionately affect the outcomes.

In every model, the prosthetic crown was designed so that the distance from its upper surface to the implant platform was 12 mm. Since loading was applied 1 mm below the cusp tip, the effective vertical distance between the loading point and the implant platform was 11 mm **(Figure 3)**.

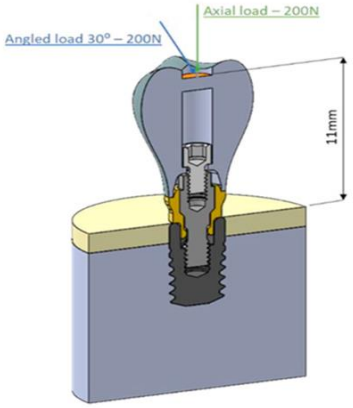

Figure 3. Load application zones: orange = applied area, green = 200 N axial force, blue = 200 N angled at 30°.

BTI "Core" narrow internal connection implants (BTI Biotechnology Institute, Vitoria, Spain) were selected for all models, with diameters Ø3.3, Ø3.5, Ø3.75, Ø4.0, Ø4.25, and Ø4.75 mm, and a uniform length of 6.5 mm. A 2-mm Multi-Im transepithelial intermediate abutment (BTI Biotechnology Institute, Vitoria, Spain) was incorporated in each case. The mechanical features of the modeled materials are shown in **Table 1**.

The geometry of all components was created in SolidWorks Professional 2020 (Dassault Systèmes®, Vélizy-Villacoublay, France) according to manufacturer data. Finite element meshing was performed using SolidWorks Simulation Premium 2020 with 10-node tetrahedral elements and a maximum element size of 0.2 mm **(Figure 4)**. Previous studies have verified that an element size smaller than 0.3 mm provides sufficient accuracy at the bone–implant interface [19].

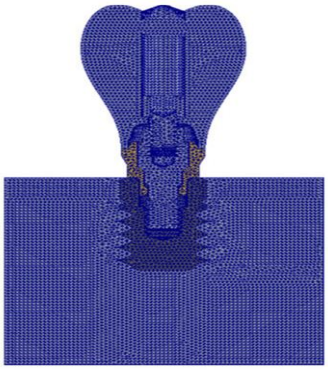

Figure 4. Meshed finite element model.

Material properties were defined as homogeneous, isotropic, and linearly elastic. All interfaces were assigned as rigid connections with compatible meshes to represent full osseointegration. Boundary conditions restricted all movements along the external bone surfaces, and symmetry was maintained throughout the model. A uniformly distributed load of 200 N [20, 21] was applied vertically or at a 30° inclination to the upper face of the prosthesis, positioned 11 mm above the bone surface **(Figure 4)**.

Table 1. Mechanical parameters of materials used in finite element modeling.

Component	Material	Young's Modulus (MPa)	Poisson's Ratio
Dental Implant	Commercially Pure Titanium [22]	105,000	0.37
Prosthesis Screw	Titanium Alloy [22]	113,800	0.342
Transepithelial Body	Commercially Pure Titanium [22]	105,000	0.37
Transepithelial Screw	Titanium Alloy [22]	113,800	0.342

Prosthesis	Co-Cr Alloy [20]	218,000	0.33
Cortical Bone	Cortical Bone [20]	13,700	0.28
Cancellous Bone	Cancellous Bone [20]	1,370	0.3

Results and Discussion

Upon assessing implant performance across the four bone classifications and two loading scenarios, the highest Von Mises equivalent stress values in the bone, as well as their surrounding distribution, were determined.

Table 2 presents the maximum Von Mises stress in bone under a 200 N axial load, whereas **Table 3** reports the corresponding values for a 30° oblique load. It was evident that stresses induced by the angled load were markedly greater than those generated under axial loading conditions.

Table 2. Peak Von Mises equivalent stress (MPa) in bone under a 200 N axial load.

Implant Diameter (mm)	Ø3.3	Ø3.5	Ø3.75	Ø4	Ø4.25	Ø4.75
Bone Quality Type IV	235	215	125	102	90	68
Bone Quality Type III	230	205	120	90	83	60
Bone Quality Type II	205	190	110	82	71	52
Bone Quality Type 0-I	180	173	97	69	58	41

Table 3. Peak Von Mises equivalent stress (MPa) in bone under a 30° oblique load of 200 N.

Implant Diameter (mm)	Ø3.3	Ø3.5	Ø3.75	Ø4	Ø4.25	Ø4.75
Bone Quality Type IV	40	39	22	19.5	17	16
Bone Quality Type III	39	38	23	19.5	17	15
Bone Quality Type II	33	32	19	16	14	11
Bone Quality Type 0-I	21	20	10.5	8.5	7.5	5.5

An increase in bone density resulted in a noticeable reduction of stress within the surrounding bone tissue. The stress decrease ranged from 48–66% for axially loaded implants and 23–40% for obliquely loaded implants. Implant diameter also influenced the stress distribution pattern: for the same bone category, smaller-diameter implants produced up to fourfold higher bone stress than wider ones.

Figure 5 displays the maximum Von Mises stress values for all test conditions under axial loading, while **Figure 6** illustrates those obtained under angled loading.

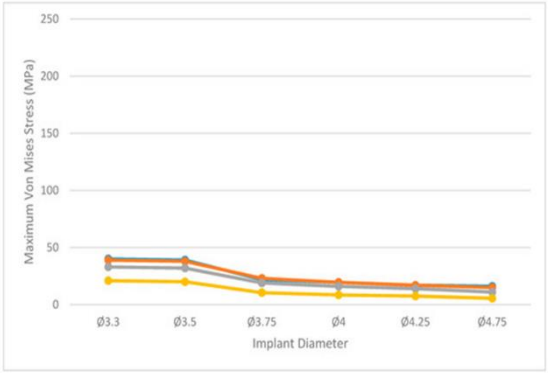

Figure 5. Maximum equivalent Von Mises stress (MPa) in bone under a 200 N axial load for Bone types 0–I (yellow), II (grey), III (orange), and IV (blue).

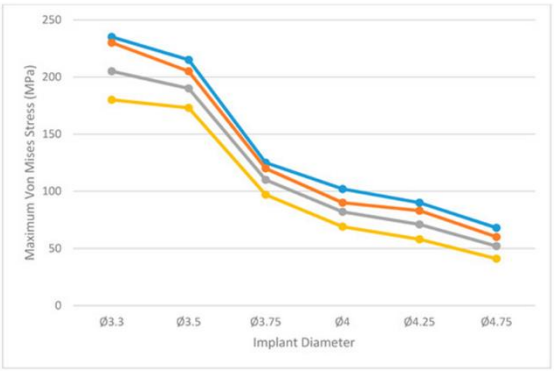

Figure 6. Maximum equivalent Von Mises stress (MPa) in bone under a 30° angled load of 200 N for Bone types 0–I (yellow), II (grey), III (orange), and IV (blue).

Figures 7–12 depict the spatial Von Mises stress distribution in bone for each implant configuration analyzed.

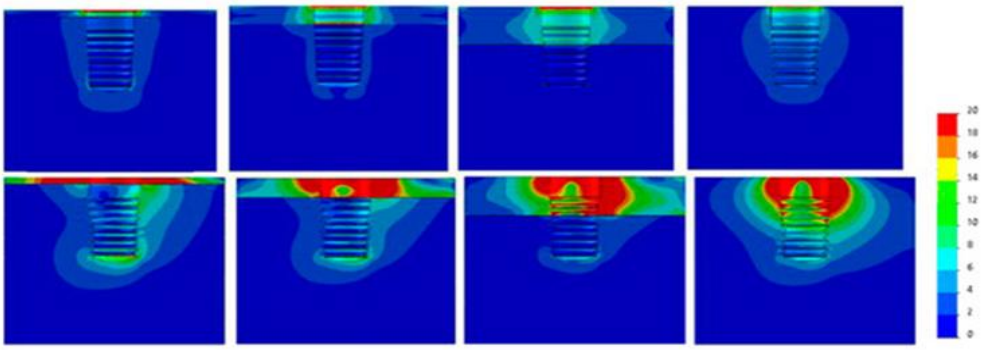

Figure 7. Ø3.3 mm implant – axial (top) and angled (bottom) loads; bone types IV → 0–I (left → right).

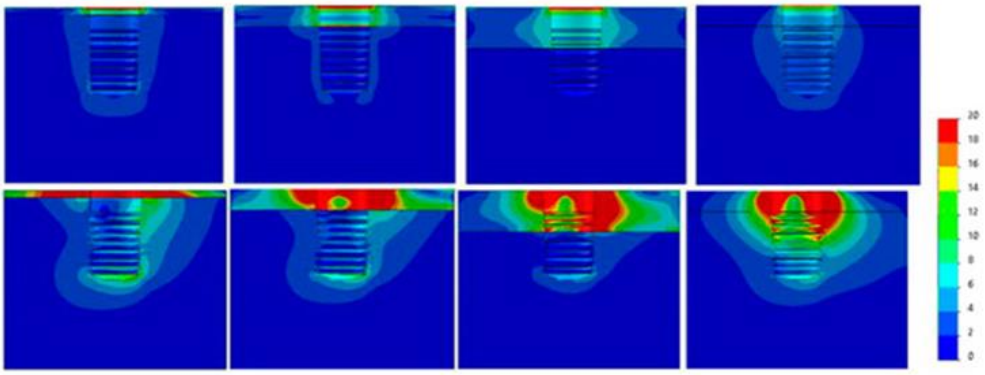

Figure 8. Ø3.5 mm implant – axial (top) and angled (bottom) loads; bone types IV → 0–I (left → right).

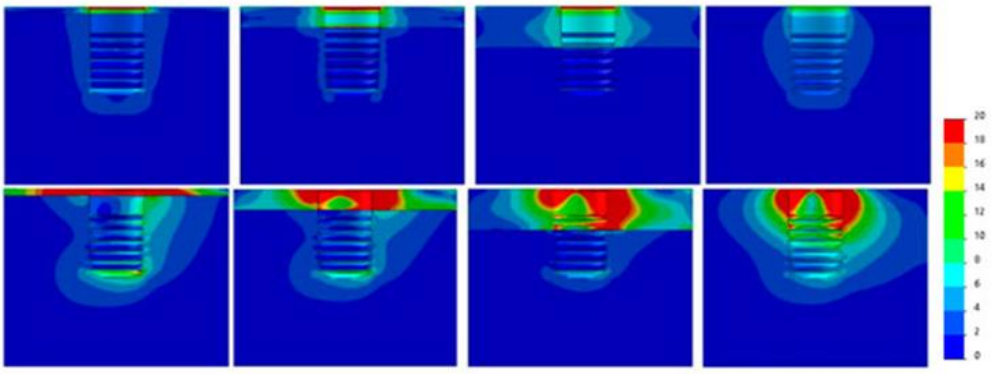

Figure 9. Ø3.75 mm implant – axial (top) and angled (bottom) loads; bone types IV → 0–I (left → right).

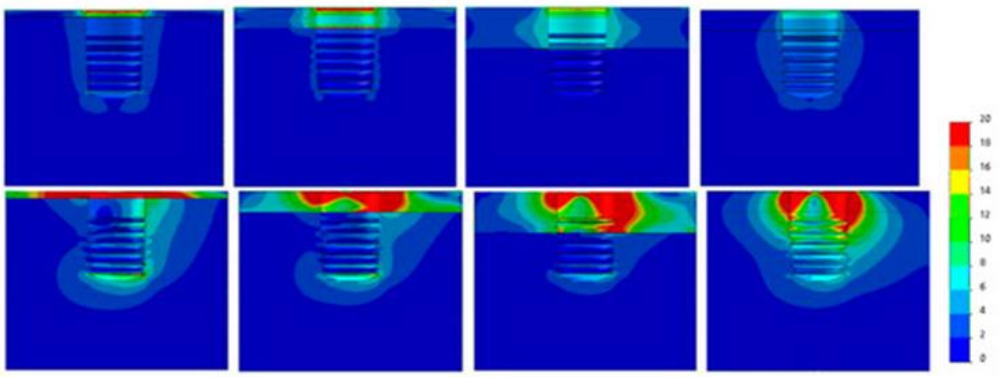

Figure 10. Ø4.0 mm implant – axial (top) and angled (bottom) loads; bone types IV → 0–I (left → right).

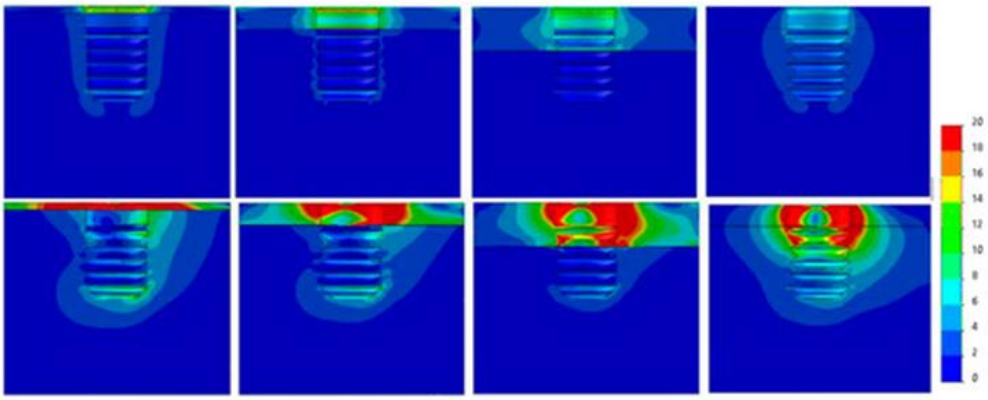

Figure 11. Ø4.25 mm implant – axial (top) and angled (bottom) loads; bone types IV → 0–I (left → right).

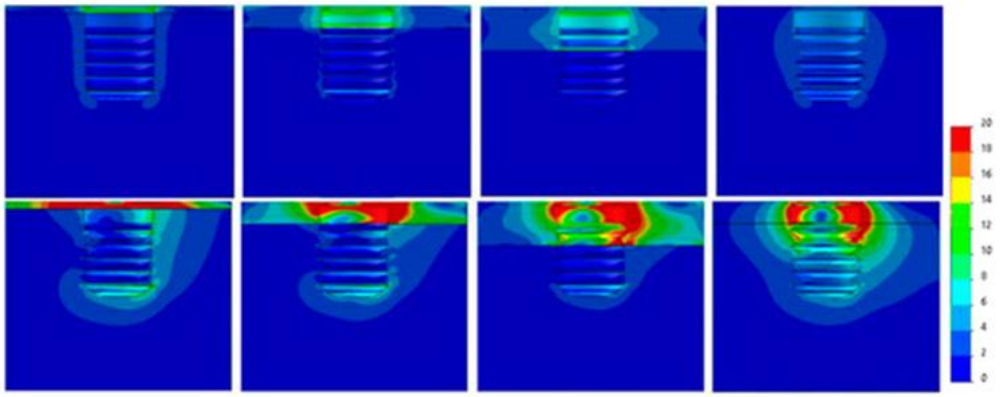

Figure 12. Ø4.75 mm implant – axial (top) and angled (bottom) loads; bone types IV → 0–I (left → right).

The success of implant therapy relies heavily on how mechanical loads are transmitted to the supporting bone structure. This stress transfer is influenced by multiple variables, including loading direction, implant geometry, and bone quality. The finite element method (FEM) enables simulation and prediction of such stress behavior in both the implant and peri-implant bone [1]. Under axial load, the maximum stress observed in bone reached 40 MPa, corresponding to Type IV bone with the narrowest Ø3.3 mm implant. Conversely, the lowest stress occurred in the highest-density bone (Type 0–I) using the Ø4.75 mm implant. Incremental increases in implant width consistently lowered bone stress, and similar trends were noted as bone density improved. These findings are comparable to those reported by Azcarate-Velázquez *et al*. [12]. Notably, for axial loading, no clear difference was detected between Types III and IV bone, though the stress reduction effect was more pronounced among the denser categories.

The region near the implant collar consistently exhibited the greatest stress concentration—an outcome also documented by Eazhil *et al*. [9].

In the oblique loading condition, the maximum stress (235 MPa) occurred with the Ø3.3 mm implant in Type IV bone, while the lowest stress (41 MPa) was associated with the Ø4.75 mm implant in Type 0–I bone. As implant diameter increased, stress in the bone decreased accordingly. These outcomes align with earlier studies [5, 9], which concluded that larger-diameter implants more effectively distribute mechanical forces, thereby reducing peri-implant bone stress.

In the current investigation, the use of an implant with a Ø3.3 mm diameter produced 2.5 to 4.4 times higher stress compared to a Ø4.75 mm diameter implant, depending on the bone type. It has been demonstrated that implant diameter plays a key role in determining the stress concentration within the bone adjacent to the implant, thereby influencing the implant's survival rate [23]. Increasing the implant's diameter can lower both implant and peri-implant bone stress, a phenomenon attributed to improved load distribution resulting from the expanded contact interface between the implant and bone [24, 25]. Furthermore, a greater implant diameter tends to enhance primary stability. This initial stability is affected by factors such as bone density, implant geometry, and the diametral ratio between the prepared socket and the implant body [26, 27].

However, it should be emphasized that while larger diameters reduce bone stress, this does not automatically guarantee higher success rates, since outcomes depend on several additional factors beyond mechanical stress alone. Moreover, wider implants demand greater bone volume, which may not always be available. Supporting this, Krennmair *et al*. reported no significant variation in success rates among implants of different diameters in their analysis [28].

It is also worth noting that angled loading consistently generated substantially higher stresses than axial loading. In the case of the Ø3.75 mm implant within Type 0–I bone, stress levels were observed to be nine times greater under oblique loading. These findings agree with Sesha *et al*., who reported increased bone stress when the load was applied at a 30° inclination rather than vertically [29]. Similarly, Papavasiliou *et al*. determined that oblique forces produced stresses nearly tenfold higher than axial forces [30]. In a theoretical evaluation, Rangert *et al*. also indicated that axial forces are more favorable, while bending moments impose greater stress on both the implant and surrounding bone [31].

Lastly, it must be recognized that finite element modeling (FEM) serves only as an approximation of real biomechanical conditions. These analyses represent a simplified virtual simulation of three-dimensional structures [21]. The assumptions used in the modeling—such as isotropic material properties, boundary condition constraints, and contact behavior—may influence the numerical outcomes. Nevertheless, since identical simplifications were applied across all models, valid comparative evaluations between scenarios remain possible. To further substantiate these findings, clinical validation through in vivo studies is recommended.

Conclusion

Enhanced bone quality correlates with reduced stress levels in the bone structure. A comparable, though more pronounced, reduction occurs with larger implant diameters. The increase in stress caused by narrower implants under axial loads is significantly lower than that observed under oblique loading. Consequently, for single-unit restorations—particularly in the molar region—it is advisable to utilize wider implants, especially when bone density is low. A comprehensive understanding of stress distribution patterns can guide clinicians in selecting the appropriate implant diameter based on anatomical and bone quality considerations.

Acknowledgments: None

Conflict of Interest: None

Financial Support: None

Ethics Statement: None

References

1. Geng JP, Tan KBC, Liu GR. Application of finite element analysis in implant dentistry: a review of the literature. J Prosthet Dent. 2001;85(6):585–98.
2. Anitua E. The biomechanics of the short implant. In: Anitua E, ed. Short and Extra-Short Implants. Vitoria (Spain): Team Work Media España; 2017. 57 p.
3. Huang HL, Hsu JT, Fuh LJ, Tu MG, Ko CC, Shen YW. Bone stress and interfacial sliding analysis of implant designs on an immediately loaded maxillary implant: a non-linear finite element study. J Dent. 2008;36(6):409–17.
4. Baggi L, Cappelloni I, Di Girolamo M, Maceri F, Vairo G. The influence of implant diameter and length on stress distribution of osseointegrated implants related to crestal bone geometry: a three-dimensional finite element analysis. J Prosthet Dent. 2008;100(6):422–31.
5. Anitua E, Tapia R, Luzuriaga F, Orive G. Influence of implant length, diameter, and geometry on stress distribution: a finite element analysis. Int J Periodontics Restor Dent. 2010;30(1):89–95.
6. Urdaneta RA, Leary J, Lubelski W, Emanuel KM, Chuang SK. The effect of implant size 5×8 mm on crestal bone levels around single-tooth implants. J Periodontol. 2012;83(10):1235–44.
7. Nissan J, Ghelfan O, Gross O, Priel I, Gross M, Chaushu G. The effect of crown/implant ratio and crown height space on stress distribution in unsplinted implant supporting restorations. J Oral Maxillofac Surg. 2011;69(7):1934–9.
8. Dos LP, Renouard F, Renault P, Barquins M. Influence of implant length and bicortical anchorage on implant stress distribution. Clin Implant Dent Relat Res. 2003;5(4):254–62.
9. Eazhil R, Swaminathan SV, Gunaseelan M, Kannan GV, Alagesan C. Impact of implant diameter and length on stress distribution in osseointegrated implants: a 3D FEA study. J Int Soc Prev Community Dent. 2016;6(6):590–6.
10. Anitua E, Alkhraisat M, Piñas L, Orive G. Efficacy of biologically guided implant site preparation to obtain adequate primary implant stability. Ann Anat. 2015;199:9–15.

11. Rabel A, Köhler SG, Schmidt-Westhausen AM. Clinical study on the primary stability of two dental implant systems with resonance frequency analysis. Clin Oral Investig. 2007;11(3):257–65.
12. Velazquez FA, Castillo-Oyagüe R, Oliveros-López LG, Torres-Lagares D, Martínez-González ÁJ, Pérez-Velasco A, et al. Influence of bone quality on the mechanical interaction between implant and bone: a finite element analysis. J Dent. 2019;88:103161.
13. Anitua E, Alkhraisat M. Clinical performance of short dental implants supporting single crown restoration in the molar-premolar region: cement versus screw retention. Int J Oral Maxillofac Implants. 2019;34(4):969–76.
14. Guljé FL, Raghoebar GM, Vissink A, Meijer HJA. Single crowns in the resorbed posterior maxilla supported by either 6-mm implants or by 11-mm implants combined with sinus floor elevation surgery: a 1-year randomized controlled trial. Eur J Oral Implantol. 2014;7(3):247–55.
15. Mezzomo LA, Miller R, Triches D, Alonso F, Shinkai R. Meta-analysis of single crowns supported by short (<10 mm) implants in the posterior region. J Clin Periodontol. 2014;41(2):191–213.
16. Meijer HJA, Boven C, Delli K, Raghoebar GM. Is there an effect of crown-to-implant ratio on implant treatment outcomes? A systematic review. Clin Oral Implants Res. 2018;29(Suppl 18):243–52.
17. Guljé FL, Raghoebar GM, Al Erkens W, Meijer HJ. Impact of crown-implant ratio of single restorations supported by 6-mm implants: a short-term case series study. Int J Oral Maxillofac Implants. 2016;31(3):672–5.
18. Lekholm UZG. Patient selection and preparation. In: Zarb GA, Brånemark PI, Alberktsson T, eds. Tissue-Integrated Prostheses: Osseointegration in Clinical Dentistry. Chicago (IL): Quintessence Publishing; 1985. p. 199–209.
19. Sato Y, Teixeira E, Tsuga K, Shindoi N. The effectiveness of a new algorithm on a three-dimensional finite element model construction of bone trabeculae in implant biomechanics. J Oral Rehabil. 1999;26(8):640–3.
20. Capatti RS, Barboza MS, Antunes ANDG, Oliveira DD, Seraidarian PI. Viability of maxillary single crowns supported by 4-mm short implants: a finite element study. Int J Oral Maxillofac Implants. 2020;35(6):e41–e50.
21. Doganay O, Kilic E. Comparative finite element analysis of short implants with different treatment approaches in the atrophic mandible. Int J Oral Maxillofac Implants. 2020;35(6):e69–e76.
22. Moreira de Melo EJ Jr, Francischone CE. Three-dimensional finite element analysis of two angled narrow-diameter implant designs for an all-on-4 prosthesis. J Prosthet Dent. 2020;124(4):477–84.
23. Akça K, Iplikçioğlu H. Finite element stress analysis of the influence of staggered versus straight placement of dental implants. Int J Oral Maxillofac Implants. 2001;16(5):722–30.
24. Okumura N, Stegaroiu R, Kitamura E, Kurokawa K, Nomura S. Influence of maxillary cortical bone thickness, implant design and implant diameter on stress around implants: a three-dimensional finite element analysis. J Prosthodont Res. 2010;54(3):133–42.
25. Qian L, Todo M, Matsushita Y, Koyano K. Effects of implant diameter, insertion depth, and loading angle on stress/strain fields in implant/jawbone systems: Finite element analysis. Int J Oral Maxillofac Implants. 2009;24(5):877–86.
26. Barewal RM, Stanford C, Weesner TC. A randomized controlled clinical trial comparing the effects of three loading protocols on dental implant stability. Int J Oral Maxillofac Implants. 2012;27(5):945–56.
27. Nevins M, Nevins ML, Schupbach P, Fiorellini J, Lin Z, Kim DM. The impact of bone compression on bone-to-implant contact of an osseointegrated implant: a canine study. Int J Periodontics Restor Dent. 2012;32(6):637–45.
28. Krennmair G, Seemann R, Schmidinger S, Ewers R, Piehslinger E. Clinical outcome of root-shaped dental implants of various diameters: 5-year results. Int J Oral Maxillofac Implants. 2010;25(2):357–66.
29. Sesha MR, Sunduram R, Abdelmagyd HAE. Biomechanical evaluation of stress distribution in subcrestal placed platform-switched short dental implants in D4 bone: in vitro finite-element model study. J Pharm Bioallied Sci. 2020;12(Suppl 1):S134–9.
30. Papavasiliou G, Kamposiora P, Bayne SC, Felton DA. Three-dimensional finite element analysis of stress distribution around single tooth implants as a function of bony support, prosthesis type, and loading during function. J Prosthet Dent. 1996;76(6):633–40.
31. Rangert B, Jemt T, Jörneus L. Forces and moments on Brånemark implants. Int J Oral Maxillofac Implants. 1989;4(3):86–104.